
Interpreting Blackbox Models via Model Extraction

Osbert Bastani¹ Carolyn Kim² Hamsa Bastani¹

Abstract

Interpretability has become incredibly important as machine learning is increasingly used to inform consequential decisions. We propose to construct *global explanations* of complex, blackbox models in the form of a decision tree approximating the original model—as long as the decision tree is a good approximation, then it mirrors the computation performed by the blackbox model. We devise a novel algorithm for extracting decision tree explanations that actively samples new training points to avoid overfitting. We evaluate our algorithm on a random forest to predict diabetes risk and a learned controller for cart-pole. Compared to several baselines, our decision trees are both substantially more accurate and equally or more interpretable based on a user study. Finally, we describe several insights provided by our interpretations, including a causal issue validated by a physician.

1. Introduction

Machine learning has revolutionized our ability to use data to inform critical decisions, such as medical diagnosis (Kononenko, 2001; Caruana et al., 2015; Valdes et al., 2016), bail decisions for defendants (Kleinberg et al., 2017; Jung et al., 2017) and the design of aircraft collision avoidance systems (Temizer et al., 2010). At the same time, machine learning models have been shown to exhibit unexpected defects when deployed in the real world, such as causality issues (i.e., inability to distinguish causal effects from correlations) (Pearl, 2009; Caruana et al., 2015), fairness (i.e., internalizing prejudices present in training data) (Dwork et al., 2012; Hardt et al., 2016), and covariate shift (i.e., differences in the training and test distributions) (Shimodaira, 2000; Candela et al., 2009).

Interpretability is a promising way to address these challenges (Rudin, 2014; Doshi-Velez & Kim, 2017), since it enables data scientists to diagnose issues in machine learning

models (Caruana et al., 2012; Wang & Rudin, 2015; Letham et al., 2015; Ustun & Rudin, 2016; Ribeiro et al., 2016). There are three approaches to interpretability. First, we can deploy an interpretable model such as a decision tree or a rule list in production (Caruana et al., 2012; Wang & Rudin, 2015; Letham et al., 2015; Ustun & Rudin, 2016), allowing the data scientist to validate the deployed model; however, this approach often requires sacrificing accuracy. Alternatively, we can use a complex model in production, but provide a *local explanation* for each of its predictions (Ribeiro et al., 2016); however, the data scientist must now validate each prediction made. In contrast, our approach is to extract a *global explanation* in the form of an interpretable model that approximates the complex model; as long as the approximation quality is good, then the interpretable model mirrors the computation performed by the complex model. Thus, by inspecting the interpretable model, the data scientist can diagnose issues in the complex model. To maximize applicability, we treat the complex model as a *blackbox*, i.e., we only require the ability to run the model on a chosen input and observe the corresponding output.

We use decision trees as global explanations, since they are nonparametric (so they can closely approximate complex models) but highly structured (so they are interpretable). The challenge is that decision trees are hard to learn (Frosst & Hinton, 2017). We propose a *model extraction* algorithm for learning decision trees—to avoid overfitting, our algorithm generates new training data by actively sampling new inputs and labeling them using the complex model. We evaluate our algorithm on two benchmarks: a random forest trained to predict diabetes risk and a control policy for cart-pole (Barto et al., 1983). We find that our decision trees are substantially more accurate (relative to the complex model) compared to several baselines. An important question is whether decision trees are interpretable. A key contribution of our work is a user study evaluating interpretability by asking machine learning graduate students to perform tasks such as computing counterfactuals and identifying risky subpopulations; we find that our decision trees are equally or more interpretable compared to the baselines. Finally, we describe several insights based on our interpretations, including a causal issue validated by a physician.

¹University of Pennsylvania ²Stanford University. Correspondence to: Osbert Bastani <obastani@seas.upenn.edu>.

Related work. There has been much interest in learning interpretable models, including decision trees (Breiman et al., 1984), rule lists (Wang & Rudin, 2015; Letham et al., 2015), sparse linear models (Tibshirani, 1996; Ustun & Rudin, 2016; Jung et al., 2017), generalized additive models (Caruana et al., 2012), and decision sets (Lakkaraju et al., 2016). There has been work using model compression (Bucilua et al., 2006) to learn decision trees (Breiman & Shang, 1996; Frosst & Hinton, 2017), but they use rejection sampling, whereas our active sampling strategy directly targets paths most in need of additional data, thereby substantially improving accuracy. There have also been approaches focused on extracting decision trees from specific model families such as random forests (Van Assche & Blockeel, 2007; Deng, 2014; Vandewiele et al., 2016); in contrast, our approach is fully blackbox, enabling it to work with any model family. There has been work on constructing global explanations: *relative influence* scores the contribution of each feature in random forests (Friedman, 2001), and (Datta et al., 2016) uses the Shapley value to quantify feature influence. In recent work, (Lakkaraju et al., 2017) extracts global explanations in the form of decision sets; we show that our decision trees are equally interpretable while achieving higher accuracy relative to the complex model.

2. Problem Formulation

Our algorithm learns axis-aligned decision trees (Breiman et al., 1984). An *axis-aligned constraint* is a constraint $C = (x_i \leq t)$, where $i \in [d] = \{1, \dots, d\}$ and $t \in \mathbb{R}$, where d is the dimension of the input space \mathcal{X} . More general constraints can be built from existing constraints using negations $\neg C$, conjunctions $C_1 \wedge C_2$, and disjunctions $C_1 \vee C_2$. The *feasible set* of C is $\mathcal{F}(C) = \{x \in \mathcal{X} \mid x \text{ satisfies } C\}$.

A *decision tree* T is a binary tree. An *internal node* $N = (N_L, N_R, C)$ of T has a left child node N_L and a right child node N_R , and is labeled with an axis-aligned constraint $C = (x_i \leq t)$. A *leaf node* $N = (y)$ of T is associated with a label $y \in \mathcal{Y}$. We use N_T to denote the root node of T . The decision tree is interpreted as a function $T : \mathcal{X} \rightarrow \mathcal{Y}$ in the usual way. More precisely, a leaf node $N = (y)$ is interpreted as a function $N(x) = y$, an internal node $N = (N_L, N_R, C)$ is interpreted as a function $N(x) = N_L(x)$ if $x \in \mathcal{F}(C)$, and $N(x) = N_R(x)$ otherwise. Then, $T(x) = N_T(x)$. For a node $N \in T$, we let C_N denote the conjunction of the constraints along the path from the root of T to N . More precisely, C_N is defined recursively: for the root N_T , we have $C_{N_T} = \text{True}$, and for an internal node $N = (N_L, N_R, C)$, we have $C_{N_L} = C_N \wedge C$ and $C_{N_R} = C_N \wedge \neg C$.

Given a training set $X_{\text{train}} \subseteq \mathcal{X}$ and blackbox access to a function $f : \mathcal{X} \rightarrow \mathcal{Y}$, our goal is to learn a decision tree $T : \mathcal{X} \rightarrow \mathcal{Y}$ that approximates f . We focus on the case

$\mathcal{X} = \mathbb{R}^d$ and $\mathcal{Y} = [m]$ (i.e., classification); our approach easily generalizes to the case where \mathcal{X} contains categorical dimensions, and to $\mathcal{Y} = \mathbb{R}$ (i.e., regression). For classification, we measure performance using accuracy relative to f on a held out test set, i.e., $\frac{1}{|X_{\text{test}}|} \sum_{x \in X_{\text{test}}} \mathbb{I}[T(x) = f(x)]$. For binary classification, we use F_1 score, and for regression, we use mean-squared error.

3. Decision Tree Extraction Algorithm

Our algorithm first uses X_{train} to estimate a distribution \mathcal{P} over \mathcal{X} . For scalability, our algorithm greedily constructs the decision tree T : it initializes T to a single leaf (the root), and then iteratively splits leaf nodes in T . To split a leaf $N \in T$, it uses an active sampling strategy to sample new inputs $x \sim \mathcal{P}$ such that $x \in \mathcal{F}(C_N)$, computes the corresponding labels $y = f(x)$, and uses this data to identify the best split. We first describe the *exact greedy decision tree* T^* , i.e., the decision tree extracted using infinite data, and then describe how our algorithm estimates T^* .

Input distribution. We fit a mixture of axis-aligned Gaussians to X_{train} using EM. The categorical distribution over mixtures is $j \sim \text{Categorical}(\phi)$ (where $\phi \in \mathbb{R}^k$), and the mixture distributions are $x \sim \mathcal{N}(\mu_j, \Sigma_j)$ for each $j \in [K]$ (where $\mu \in \mathbb{R}^{Kd}$ and $\Sigma \in \mathbb{R}^{Kd^2}$, and each Σ_j is diagonal).

Exact greedy decision tree. We construct the *exact greedy decision tree* T^* of size k similar to CART (Breiman et al., 1984). We initialize T^* to a single leaf $N_{T^*} = (y)$, where y is the majority label according to \mathcal{P} . Then, we iteratively split leaves in T^* (using a total of $k - 1$ iterations)—at each iteration, we choose a leaf $N = (y)$ in T^* and replace it with an internal node $N' = (N_L, N_R, C)$, where $N_L = (y_L)$ and $N_R = (y_R)$ are new leaf nodes, and $C = (x_{i^*} \leq t^*)$, where

$$(i^*, t^*) = \arg \max_{i \in [d], t \in \mathbb{R}} G(i, t), \quad (1)$$

where the gain

$$\begin{aligned} G(i, t) &= -H(f, C_N \wedge (x_i \leq t)) \\ &\quad - H(f, C_N \wedge (x_i > t)) + H(f, C_N) \\ H(f, C) &= \left(1 - \sum_{y \in \mathcal{Y}} \Pr_{x \sim \mathcal{P}}[f(x) = y \mid C]^2\right) \cdot \Pr_{x \sim \mathcal{P}}[C] \end{aligned} \quad (2)$$

uses the (weighted) Gini impurity H (other metrics can be used as well). The leaf node labels are

$$y_L = \arg \max_{y \in \mathcal{Y}} \Pr_{x \sim \mathcal{P}}[f(x) = y \mid C_N \wedge (x_i \leq t)] \quad (3)$$

$$y_R = \arg \max_{y \in \mathcal{Y}} \Pr_{x \sim \mathcal{P}}[f(x) = y \mid C_N \wedge (x_i > t)].$$

We choose to replace the leaf $N \in T^*$ with the highest gain (2); we terminate early if its gain is zero.

Interpreting Blackbox Models via Model Extraction

Dataset	Task	# Features	Outcomes	# Training	# Test	Blackbox Model	Blackbox Performance
diabetes risk	classification	384	{high risk, low risk}	404	174	random forest	$F_1 = 0.24$
cart-pole (Barto et al., 1983)	reinforcement learning	4	{left, right}	100	100	control policy	reward = 200.0

Table 1. Summary of the datasets used in our evaluation.

Estimated greedy decision tree. Given $n \in \mathbb{N}$, our algorithm constructs a greedy decision tree \hat{T} in the same way as the construction of T^* , except (2) and (3) are estimated using n i.i.d. samples $x \sim \mathcal{P} \mid C_N$ each (we select which leaf $N \in T^*$ to expand using n additional samples). We describe how to sample $x \sim \mathcal{P} \mid C$, where C is a conjunction of axis-aligned constraints

$$C = (x_{i_1} \leq t_1) \wedge \dots \wedge (x_{i_k} \leq t_k) \\ \wedge (x_{j_1} > s_1) \wedge \dots \wedge (x_{j_h} > s_h).$$

Constraints in C may be redundant—(i) for two constraints $x_i \leq t$ and $x_i \leq t'$ such that $t \leq t'$, the first constraint implies the second, so we can discard the latter, and (ii) for two constraints $x_i > s$ and $x_i > s'$ such that $s \geq s'$, we can similarly discard the latter. Given two constraints $x_i \leq t$ and $x_i > s$, we can assume that $t \geq s$ (otherwise C is unsatisfiable, so the gain (2) is zero and the algorithm terminates). In summary, we can assume C contains at most one inequality ($x_i \leq t$) and at most one inequality ($x_i > s$) for each $i \in [d]$, and if both are present, then the two are not mutually exclusive. For simplicity, we assume C contains both inequalities for each $i \in [d]$:

$$C = (s_1 \leq x_1 \leq t_1) \wedge \dots \wedge (s_d \leq x_d \leq t_d).$$

Now, recall that \mathcal{P} is a mixture of axis-aligned Gaussians, so it has probability density function

$$p_{\mathcal{P}}(x) = \sum_{j=1}^K \phi_j \cdot p_{\mathcal{N}(\mu_j, \Sigma_j)}(x) \\ = \sum_{j=1}^K \phi_j \prod_{i=1}^d p_{\mathcal{N}(\mu_{ji}, \sigma_{ji})}(x_i),$$

where $\sigma_{ji} = (\Sigma_j)_{ii}$. The conditional distribution is

$$p_{\mathcal{P}|C}(x) \propto \sum_{j=1}^K \phi_j \prod_{i=1}^d p_{\mathcal{N}(\mu_{ji}, \sigma_{ji})|C}(x_i) \\ = \sum_{j=1}^K \phi_j \prod_{i=1}^d p_{\mathcal{N}(\mu_{ji}, \sigma_{ji})|(s_i \leq x_i \leq t_i)}(x_i).$$

Since the Gaussians are axis-aligned, the unnormalized probability of each component is

$$\tilde{\phi}'_j = \int \phi_j \prod_{i=1}^d p_{\mathcal{N}(\mu_{ji}, \sigma_{ji})|(s_i \leq x_i \leq t_i)}(x_i) dx \\ = \phi_j \prod_{i=1}^d \left(\Phi \left(\frac{t_i - \mu_{ji}}{\sigma_{ji}} \right) - \Phi \left(\frac{s_i - \mu_{ji}}{\sigma_{ji}} \right) \right),$$

where Φ is the cumulative density function of the standard Gaussian distribution $\mathcal{N}(0, 1)$. Then, the normalization constant is $Z = \sum_{j=1}^K \tilde{\phi}'_j$, and the component probabilities are $\tilde{\phi} = Z^{-1} \tilde{\phi}'$. Finally, to sample $x \sim \mathcal{P} \mid C$, we sample $j \sim \text{Categorical}(\tilde{\phi})$, and $x_i \sim \mathcal{N}(\mu_{ji}, \sigma_{ji}) \mid (s_i \leq x_i \leq t_i)$ (for each $i \in [d]$). We use standard algorithms for sampling truncated Gaussian distributions to sample each x_i .

Theoretical guarantees. We show that $\hat{T} \rightarrow T^*$ as $n \rightarrow \infty$. A related result is (Domingos & Hulten, 2000), but their analysis is limited to discrete features, for which convergence is much easier to analyze. We give proofs in Appendix A.

Assumption 3.1. *The density $p(x)$ of \mathcal{P} is continuous, bounded ($p(x) \leq p_{max}$), and has bounded domain ($p(x) = 0$ for $|x| > x_{max}$).*

To satisfy this assumption, we can truncate our Gaussian mixture model; this modification does not affect T^* or \hat{T} very much since Gaussians have exponential tails.

Assumption 3.2. *The maximizers (i^*, t^*) in (1), and y_L and y_R in (3) are unique.*

In other words, there are no nodes where the Gini impurity for two different choices of branch are exactly tied (such a tie is very unlikely in practice); this assumption ensures that T^* is well defined. We now define the notion in which the extracted tree converges to the exact tree. For simplicity, we additionally assume that our trees are complete (i.e., have all nodes up to a given depth D).

Definition 3.3. *Let T, T' be decision trees. For any $\epsilon > 0$, we say T is an ϵ -approximation of T' if $\Pr_{x \sim \mathcal{P}}[T(x) = T'(x)] \geq 1 - \epsilon$. For any $\epsilon, \delta > 0$, we say T is (ϵ, δ) -exact if $\Pr[T \text{ is an } \epsilon \text{ approximation of } T^*] \geq 1 - \delta$ (probability over the training samples $x \sim \mathcal{P}$).*

Theorem 3.4. *For all $\epsilon, \delta > 0$, $\exists n \in \mathbb{N}$ such that \hat{T} extracted using n samples is (ϵ, δ) -exact.*

4. Evaluation

We compare the *fidelity* (i.e., accuracy relative to the complex model) and interpretability of our decision trees to several baselines on two benchmarks (see in Table 1). We also compare the fidelity of our algorithm to CART, a state-of-the-art algorithm, on a number of additional benchmarks.

Diabetes risk. The goal of this dataset is to predict whether a patient has high or low risk for type II diabetes,

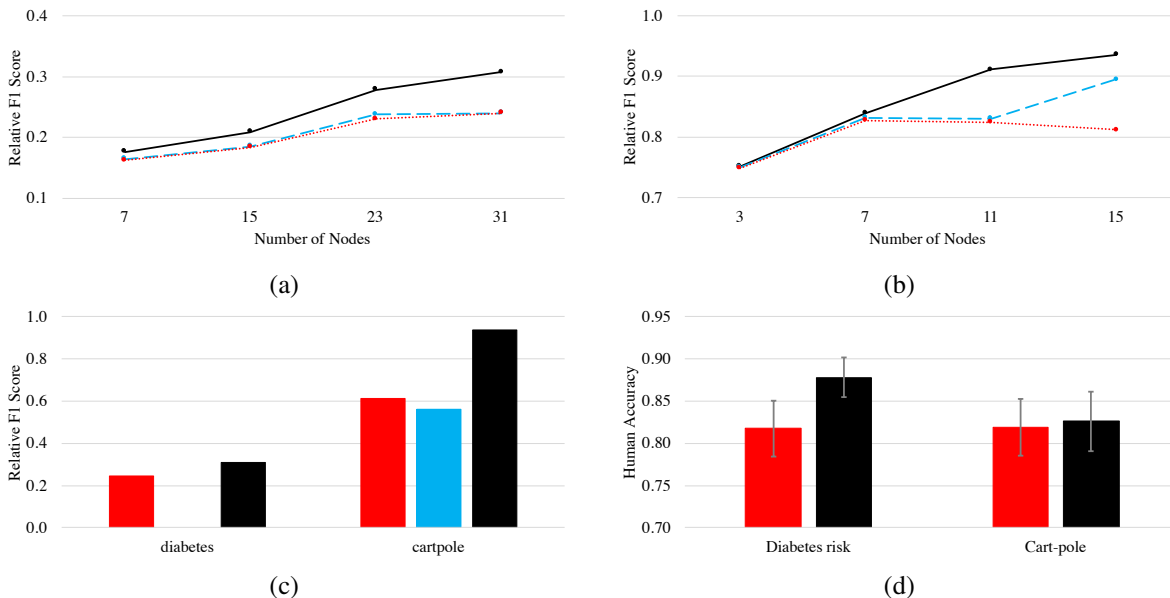


Figure 1. Fidelity on (a) the diabetes risk benchmark, and (b) the cart-pole benchmark, of decision trees learned using CART (red, dotted), the born-again algorithm (blue, dashed), and our algorithm (black, solid). (c) Fidelity of rule lists (red), decision sets (blue), and our decision trees (black); the decision set learning algorithm did not scale to the diabetes risk benchmark. (d) User response accuracy for the baseline rule list or decision set (red) and our decision trees (black).

based on their ICD-9 diagnosis codes, prescribed medications, and demographics. In part of our evaluation, we compare models trained on patients from different healthcare providers. Thus, we initially focus on the largest provider (578 patients); later, for comparison, we use another large provider (402 patients). We balance the training set (only 11.8% of patients have diabetes) and train a random forest to predict risk. We extract decision tree explanations using $n = 1000$.

Cart-pole. The goal of the cart-pole problem (Barto et al., 1983) is to balance a pole on top of a cart. We discretize the state space, estimate the transition probabilities and rewards using random samples, and use value iteration to compute the optimal policy. We extract decision tree explanations using $n = 200$ (fewer samples are needed since the dimension of \mathcal{X} is much smaller).

4.1. Fidelity

High fidelity ensures that the extracted decision tree reflects the blackbox model. We measure fidelity using F_1 score on the held-out test set $\tilde{X}_{\text{test}} = \{(x, f(x)) \mid x \in X_{\text{test}}\}$, where X_{test} is the original test set. All results are medians over 20 random train/test splits. We compare to CART trees (Breiman et al., 1984) and born-again trees (Breiman & Shang, 1996), rule lists (Letham et al., 2015; Yang et al., 2017), and decision sets (Lakkaraju et al., 2016; 2017). The born-again algorithm requires an input distribution; we use

our estimated Gaussian mixture model \mathcal{P} .

Comparison to other decision trees. In Figure 1 (a) and (b), we compare the fidelity of our decision trees to that of CART trees and born-again trees for varying sizes (i.e., total number of nodes k); we outperform both baselines in every case. For larger decision trees, our active sampling strategy greatly reduces overfitting. In contrast, the born-again algorithm is unable to generate a substantial number of new training points at deeper levels of the tree since it uses rejection sampling.

Comparison to other model families. In Figure 1 (c), we compare the fidelity of our decision trees (size 31) to rule lists (trained using (Yang et al., 2017)) and decision sets (trained using (Lakkaraju et al., 2016)). We use implementations obtained from the authors. Both require us to bin continuous features; for diabetes risk, we bin age into 7 bins, and for cart-pole, we use the discretization in our MDP. We find that (Lakkaraju et al., 2016) does not scale to the diabetes risk benchmark, likely because it has hundreds of features. Our decision tree substantially outperforms the baselines. The difference on cart-pole is especially large; we believe the difference arises since features are binned—thus, the decision tree inputs are 4 dimensional, whereas the rule list and decision set inputs are 28 dimensional, making them more likely to overfit.

Dataset	Task	Samples	Features	Model	Score of f	Fidelity (Ours)	Fidelity (CART)
breast cancer (Wolberg & Mangasarian, 1990)	classify	569	32	forest	0.966 F_1	0.957 F_1	0.945 F_1
breast cancer	classify	569	32	neural net	0.951 F_1	0.956 F_1	0.949 F_1
dermatology (Güvenir et al., 1998)	classify	366	34	forest	0.994 F_1	0.970 F_1	0.967 F_1
dermatology	classify	366	34	neural net	0.988 F_1	0.997 F_1	0.964 F_1
prostate cancer (Stamey et al., 1989)	classify	97	9	forest	0.749 F_1	0.900 F_1	0.818 F_1
prostate cancer	classify	97	9	neural net	0.723 F_1	0.842 F_1	0.820 F_1
auto mpg (Quinlan, 1993)	regress	398	8	forest	8.62 MSE	2.29 MSE	2.51 MSE
auto mpg	regress	398	8	neural net	13.77 MSE	2.37 MSE	2.59 MSE
student grade (Cortez & Silva, 2008)	regress	382	33	forest	4.47 MSE	0.40 MSE	0.64 MSE
student grade	regress	382	33	neural net	6.60 MSE	4.27 MSE	5.10 MSE
mountain car (Moore, 1990)	reinforce	100	2	control policy	$R = -140.0$	81.3%	78.6%
pendulum (ope)	reinforce	100	3	control policy	$R = -638.2$	0.56 MSE	1.66 MSE

Table 2. Comparison of our algorithm to CART. For (binary) classification, fidelity is F_1 score on the test set, and for regression, it is MSE. For reinforcement learning, fidelity is accuracy (discrete actions) or MSE (continuous actions) on the test set. On every problem instance, our algorithm outperforms CART in terms of fidelity.

Stability of decision trees. Theorem 3.4 suggests that our decision trees should become more and more stable as the number of samples $n \rightarrow \infty$. We examine whether this behavior holds empirically for decision trees extracted for the diabetes risk benchmark. In particular, we used both our algorithm and the born-again algorithm to extract 10 random decision trees T_1, \dots, T_{10} . For each pair T_k and T_h (where $k \neq h$), we count the fraction of corresponding nodes in T_k and T_h that are equal (i.e., the branches at those nodes have equal values of i and t). Then, we computed the average over possible pairs. Intuitively, this metric captures the similarity between two random extracted decision trees. This metric is 0.52 (for our algorithm) vs. 0.22 (for the born-again algorithm) when $n = 2000$, and 0.67 (for our algorithm) vs. 0.25 (for the born-again algorithm) for $n = 20000$. Thus, our algorithm produces substantially more stable trees than the born-again algorithm (since it is able to get more samples to estimate each branch).

Additional comparisons to CART. We compare the fidelity of our algorithm to CART on a range of datasets; see Figure 2 for results. We outperform CART in every problem instance.

4.2. Interpretability for Diabetes Risk

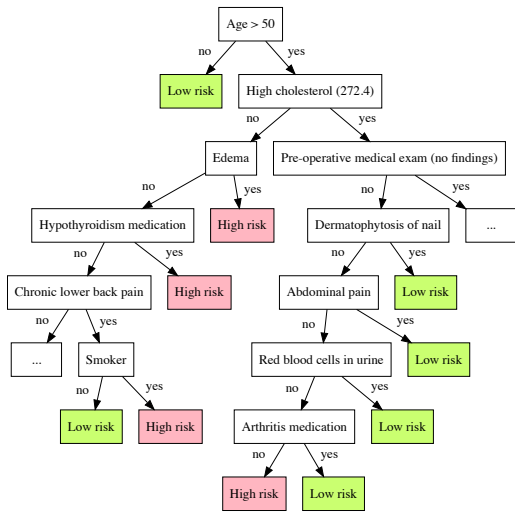
We performed a user study to evaluate the interpretability of our decision trees. Since our goal is to enable data scientists familiar with machine learning to understand and validate the complex model, we recruited 46 graduate students with a background in machine learning for our study. Each participant answered questions intended to test their understanding of various interpretations; we asked them to skip a question if they were unable to determine the answer in 1-2 minutes. We show images of our user study interface in Appendix C. We randomized the order of the models and corresponding questions. First, we describe the results for the diabetes risk benchmark.

Interpretations. We compare the two interpretations of the random forest: (i) a (randomly chosen) decision tree with 31 nodes extracted by our algorithm; a simplified version is shown in Figure 2 (a), and (ii) a rule list extracted using (Yang et al., 2017), shown in Figure 2 (c). We visualize decision trees using Graphviz, and rule lists as if-then-else programs, which is the formatting used in prior work (Yang et al., 2017) (all our users were familiar with programming). Otherwise, we tried to keep the visualizations consistent.

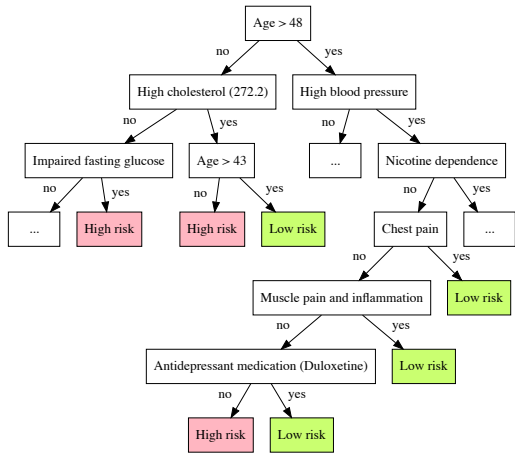
Questions. We designed five questions to test whether the user could understand an interpretable model. To ensure fairness, these questions were designed independently of the interpretations. However, we needed to adapt the questions to each of the two interpretations—in particular, we modified the possible answers to fit the structure of the interpretation so there was a single correct answer. Two examples of questions are shown in Figure 3; the variants on the left are for the decision tree, and those on the right are for the rule list. The first question tests whether the user can determine how the interpretable model classifies a given patient. The second question tests whether the user is able to identify the subpopulation for which “Smoker” is a relevant feature; enabling users to understand these subpopulation-level effects is a useful benefit of global explanations.

Results. We show user accuracies for each interpretation in Figure 1 (d) (averaged across users and questions). Users responded equally or more accurately for the decision tree, even though it is much larger than the rule list; this effect is significant ($p = 0.02$ using a paired t -test with 46 samples). For every question, a majority of users answered correctly, so we believe our questions were fair.

Difficulty with conditional structure. We found that users had difficulty understanding the conditional structure of the rule list—one of our questions required users to determine that only the first three lines of the model were relevant for patients taking arthritis medication, but only 65%



(a)



(b)

```

if Age < 41 then Low risk
else if Moderate/severe pain medication (tramadol) then High risk
else if Arthritis medication (etodolac) then Low risk
else if High cholesterol and Smoker then High risk
else if High blood pressure then High risk
else if Age < 53 then Low risk
else if Restless legs syndrome then Low risk
else if not High cholesterol then Low risk
else High risk
    
```

(c)

Figure 2. Global explanations of a risk random forest for predicting diabetes risk: (a) our decision tree, (b) our decision tree for a random forest trained on data from an alternate provider, and (c) a rule list.

of users answered correctly. For our decision tree, 91% of users correctly answered the corresponding question. This effect has also been identified in previous work (Lakkaraju et al., 2016).

Interpretation vs. blackbox model. The goal of our user study is to measure how well users can understand the interpretation. Intuitively, having high fidelity should ensure that the answers to questions according to the interpretation accurately reflect the true answers according to the blackbox model. To be sure, we evaluated how often these two answers are equal. In particular, each question in our evaluation (except question 3 on the diabetes dataset) asks for either a prediction (e.g., “Are patients age ≥ 41 classified as high risk?”) or a counterfactual (e.g., “For a smoker age ≥ 41 who is a smoker, does an intervention that gets them to quit smoking reduce diabetes risk?”). For a prediction, we compute the true answer according to the blackbox model using the formula

$$y = \arg \max_{y \in \mathcal{Y}} \Pr_{x \sim \mathcal{P}} [f(x) = y \mid C],$$

where f is the blackbox model and C is the condition on x (e.g., age ≥ 41). Similarly, for a counterfactual, we use the formula

$$\mathbb{E}_{x \sim \mathcal{P}} [f(x) \mid C, \text{do}(C')] - \mathbb{E}_{x \sim \mathcal{P}} [f(x) \mid C] \stackrel{?}{\leq} 0,$$

where C is the condition (e.g., age $\geq 41 \wedge \text{smoker} = \text{true}$) and C' is the counterfactual (e.g., $\text{do}(\text{smoker} = \text{false})$). Of the 4 questions regarding the diabetes dataset (since we omit question 3), all 4 of the answers according to the decision tree matched the true answer, whereas only 3 of the answers according to the rule list matched.

4.3. Discussion of the Diabetes Risk Classifier

Variations across providers. We can use interpretations to understand differences in random forests trained on patients from different providers. In Figure 2 (b), we show a decision tree trained on data from an alternate provider, which contained EMRs for 402 patients. We can immediately identify differences in how diagnoses were reported. For example, there are several ICD-9 codes corresponding to high cholesterol; for the original provider, 30% of patients were diagnosed with 272.4 (“unspecified hyperlipidemia”), whereas only 2% of patients were diagnosed with 272.2 (“mixed hyperlipidemia”). In contrast, for the alternate provider, 19% of patients were diagnosed with 272.2, and 18% of patients were diagnosed with 272.4. As another example, for the alternate provider, 10% of patients were diagnosed with “Impaired fasting glucose”, which appears in Figure 2 (c). In contrast, for the original provider, only 1% of patients have this diagnosis; indeed, this feature never shows up in interpretations for random forests trained on

Interpreting Blackbox Models via Model Extraction

Consider patients over 50 years old who are otherwise healthy and are not taking any medications. According to the decision tree, are these patients at a high risk for diabetes?

- Yes
- No

Smoking is known to increase risk of diabetes, so the local hospital has started a program to help smokers quit smoking. According to the decision tree, which patient subpopulation should we target in this program if we want to reduce diabetes risk?

- Patients over 50 years old who have high cholesterol
- Patients over 50 years old who have chronic lower back pain
- Patients over 50 years old who have high cholesterol, edema, chronic lower back pain, and who take medication for hypothyroidism

Consider patients over 53 years old who are otherwise healthy and are not taking any medications. According to the rule list, are these patients at a high risk for diabetes?

- Yes
- No

Smoking is known to increase risk of diabetes, so the local hospital has started a program to help smokers quit smoking. According to the rule list, which patient subpopulation should we target in this program if we want to reduce diabetes risk?

- Patients over 41 years old
- Patients over 41 years old who have high cholesterol
- Patients over 41 years old who have high cholesterol, and take medication for arthritis

Figure 3. Examples of questions asked in our user study on the diabetes risk benchmark, for our decision tree (left) and for the rule list (right).

patients from the original provider. Understanding such covariate shifts among the patient populations for different providers can help data scientists adapt existing models to new providers.

Dependence on previous doctor visits. A notable feature of the decision tree in Figure 2 (a) is the subtree rooted at the node labeled “Dermatophytosis of nail”. In this subtree, if the patient has any of the diagnoses listed, then the decision tree classifies the patient as low risk; otherwise, they are classified as high risk. This effect occurs across providers, e.g., in subtree rooted at “Chest pain” in Figure 2 (b). This effect is present (and statistically significant) in the data and in the random forest.

This effect is likely non-causal—in an interview with a physician, we learned that these diagnoses have no known relationship with diabetes risk. After examining the decision tree, the physician suggested a plausible explanation—patients who have these diagnoses are more likely to have visited a doctor at least once in the past year prior to their diabetes diagnosis, upon which the doctor may have recommended interventions designed to reduce the patient’s diabetes risk. In contrast, patients who have not visited a doctor in the past year may not have realized they were at high risk for diabetes, especially since this subtree is conditioned on patients who are over 50 years old and have high cholesterol, which are both known risk factors for diabetes. Indeed, we found that among patients over 50 years old with high cholesterol, diabetes risk was actually (statistically significantly) higher if the patient had zero previous doctor visits than if the patient had a single previous visit (despite the fact that we would expect patients with one previous visit to be sicker).

Understanding such non-causal effects is important (Caruana et al., 2015)—many patients in the subpopulation defined by this subtree are in particular need of preventative interventions, yet the classifier is proposing to discontinue interventions precisely for these patients—and our interpre-

tations provide a promising way to do so. We note that relative influence scores cannot identify this effect, since they do not examine patient subpopulations, and the effect only applies to the subpopulation of patients that are at least 50 years old and have high cholesterol. For example, the correlation of “Abdominal pain” with high risk is 8.1×10^{-3} ; however, conditioned on age greater than 50 and having high cholesterol, the correlation is -9.8×10^{-2} . Indeed, none of the features in this subtree appear in the top 40 relative influence scores of the random forest.

Non-monotone dependence on age. Note that age appears twice in the decision tree in Figure 2 (c). Typically, younger patients are at lower risk for diabetes; however, conditioned on being less than 48 years old and having high cholesterol, the classifier predicts higher risk for younger patients. While we cannot be certain of the cause, there are a number of possible explanations. For example, it may be the case that a diagnosis of high cholesterol in younger patients is abnormal and therefore much more indicative of high diabetes risk. Alternatively, doctors may be more likely to urge older patients with high cholesterol to take preventative measures to reduce diabetes risk.

This structure demonstrates how the decision tree can capture non-monotone dependencies on continuous features such as age. In contrast, non-monotone dependencies cannot be captured by relative influence scores. Rule lists can capture such dependencies, but their structure makes it more difficult to understand the effect—for example, to reason about the relationship between the first and sixth rules of the rule list in Figure 2 (c), we also have to reason about the four intermediate rules.

4.4. Interpretability for Cart-pole

Next, we describe the part of our user study focused on the cart-pole control policy.

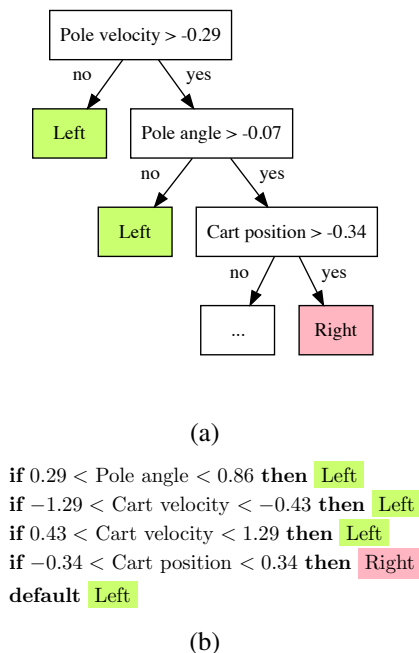


Figure 4. Global explanations of the cart-pole policy: (a) our decision tree, and (b) a decision set.

Interpretations. We compare the two interpretations of the control policy: (i) a decision tree with 15 nodes extracted using our algorithm; a simplified version is shown in Figure 4 (a), and (ii) a decision set trained using (Lakkaraju et al., 2016), shown in Figure 4 (b).

Questions. We designed three questions to check whether user could understand the interpretations. Two questions test whether the user can reason about desirable symmetries of the policy, e.g.:

In theory, the action taken should not depend on the position of the cart. Does the decision tree satisfy this property?

The third question tests whether the user can compute how the interpretation acts in given state. As for the diabetes risk benchmark, we adapt each question to each of the two interpretations.

Results. We show user accuracies for each interpretation in Figure 1 (d) (averaged across users and questions). Users responded equally or more accurately for our decision tree, even though it is larger (the difference is not statistically significant). For every question, a majority of users answered correctly, so we believe our questions were fair.

Interpretation vs. blackbox model. As with the questions about the diabetes dataset, we checked how often the answers according to the interpretation matched the true answers according to the blackbox model. In this case, for both the decision tree and the decision set, all of the answers matched.

4.5. Discussion of the Cart-Pole Controller

Translation invariance. We expect that the motion of the cart-pole should be invariant to translating the cart position. However, it is easy to see from both the decision tree and the decision set in Figure 4 that the learned policy does not exhibit this symmetry. This asymmetry likely arises because the MDP simulation always starts from a similar initial position. Thus, the cart position is highly correlated with its velocity, so the control policy can use the two interchangeably to predict what action to take. Understanding this bias in the control policy is important because it indicates that the control policy may not generalize well if the initial position changes substantially.

Reflection invariance. We also expect the motion of the cart-pole to be invariant to reflection across the y -axis (i.e., flip left and right). However, the models in Figure 4 do not exhibit this symmetry. This asymmetry likely arises because in the MDP simulation, the pole typically initially falls toward the left. Thus, to maximize performance, the control policy focuses on stopping the pole from falling toward the left, which requires moving the cart toward the left. As before, the control policy may not generalize well if we change the initial direction in which the pole is falling.

5. Conclusion

We have proposed an approach for interpreting blackbox models based on decision tree extraction, and shown how it can be used to interpret blackbox models. Important directions for future work include devising algorithms for model extraction using more expressive input distributions, and developing new ways to gain insight from the extracted decision trees.

References

- Openai pendulum-v0 environment. <https://gym.openai.com/envs/Pendulum-v0>. Accessed: 2017-05-18.
- Barto, A. G., Sutton, R. S., and Anderson, C. W. Neuronlike adaptive elements that can solve difficult learning control problems. *IEEE transactions on systems, man, and cybernetics*, 1983.
- Breiman, L. and Shang, N. Born again trees. *University*

- of California, Berkeley, Berkeley, CA, Technical Report, 1996.
- Breiman, L., Friedman, J., Stone, C. J., and Olshen, R. A. *Classification and regression trees*. CRC press, 1984.
- Bucilua, C., Caruana, R., and Niculescu-Mizil, A. Model compression. In *KDD*, 2006.
- Candela, J. Q., Sugiyama, M., Schwaighofer, A., and Lawrence, N. D. Dataset shift in machine learning, 2009.
- Caruana, R., Lou, Y., and Gehrke, J. Intelligible models for classification and regression. In *KDD*, 2012.
- Caruana, R., Lou, Y., Gehrke, J., Koch, P., Sturm, M., and Elhadad, N. Intelligible models for healthcare: Predicting pneumonia risk and hospital 30-day readmission. In *KDD*, 2015.
- Cortez, P. and Silva, A. M. G. Using data mining to predict secondary school student performance. 2008.
- Datta, A., Sen, S., and Zick, Y. Algorithmic transparency via quantitative input influence: Theory and experiments with learning systems. In *IEEE Symposium on Security and Privacy*, 2016.
- Deng, H. Interpreting tree ensembles with intrees. *arXiv:1408.5456*, 2014.
- Domingos, P. and Hulten, G. Mining high-speed data streams. In *KDD*, 2000.
- Doshi-Velez, F. and Kim, B. Towards a rigorous science of interpretable machine learning. *arXiv preprint arXiv:1702.08608*, 2017.
- Dwork, C., Hardt, M., Pitassi, T., Reingold, O., and Zemel, R. Fairness through awareness. In *ITCS*, 2012.
- Friedman, J. H. Greedy function approximation: a gradient boosting machine. *Annals of statistics*, pp. 1189–1232, 2001.
- Frosst, N. and Hinton, G. Distilling a neural network into a soft decision tree. *arXiv preprint arXiv:1711.09784*, 2017.
- Güvenir, H. A., Demiröz, G., and Ilter, N. Learning differential diagnosis of erythematous-squamous diseases using voting feature intervals. *Artificial intelligence in medicine*, 13(3):147–165, 1998.
- Hardt, M., Price, E., Srebro, N., et al. Equality of opportunity in supervised learning. In *NIPS*, 2016.
- Jung, J., Concannon, C., Shroff, R., Goel, S., and Goldstein, D. Simple rules for complex decisions. *arXiv:1702.04690*, 2017.
- Kleinberg, J., Lakkaraju, H., Leskovec, J., Ludwig, J., and Mullainathan, S. Human decisions and machine predictions. Technical report, National Bureau of Economic Research, 2017.
- Kononenko, I. Machine learning for medical diagnosis: history, state of the art and perspective. *Artificial Intelligence in medicine*, 2001.
- Lakkaraju, H., Bach, S. H., and Leskovec, J. Interpretable decision sets: A joint framework for description and prediction. In *KDD*, 2016.
- Lakkaraju, H., Kamar, E., Caruana, R., and Leskovec, J. Interpretable & explorable approximations of black box models. In *FAT/ML*, 2017.
- Letham, B., Rudin, C., McCormick, T. H., Madigan, D., et al. Interpretable classifiers using rules and bayesian analysis: Building a better stroke prediction model. *The Annals of Applied Statistics*, 9(3):1350–1371, 2015.
- Moore, A. W. *Efficient Memory-based Learning for Robot Control*. PhD thesis, University of Cambridge, 1990.
- Pearl, J. *Causality*. Cambridge university press, 2009.
- Quinlan, J. R. Combining instance-based and model-based learning. In *Proceedings of the Tenth International Conference on Machine Learning*, pp. 236–243, 1993.
- Ribeiro, M. T., Singh, S., and Guestrin, C. Why should i trust you?: Explaining the predictions of any classifier. In *KDD*, 2016.
- Rudin, C. Algorithms for interpretable machine learning. In *KDD*, 2014.
- Shimodaira, H. Improving predictive inference under covariate shift by weighting the log-likelihood function. *Journal of statistical planning and inference*, 90(2):227–244, 2000.
- Stamey, T. A., Kabalin, J. N., McNeal, J. E., Johnstone, I. M., Freiha, F., Redwine, E. A., and Yang, N. Prostate specific antigen in the diagnosis and treatment of adenocarcinoma of the prostate. ii. radical prostatectomy treated patients. *The Journal of urology*, 141(5):1076–1083, 1989.
- Temizer, S., Kochenderfer, M., Kaelbling, L., Lozano-Pérez, T., and Kuchar, J. Collision avoidance for unmanned aircraft using markov decision processes. In *AIAA guidance, navigation, and control conference*, pp. 8040, 2010.
- Tibshirani, R. Regression shrinkage and selection via the lasso. *Journal of the Royal Statistical Society. Series B (Methodological)*, pp. 267–288, 1996.

- Ustun, B. and Rudin, C. Supersparse linear integer models for optimized medical scoring systems. *Machine Learning*, 102(3):349–391, 2016.
- Valdes, G., Luna, J. M., Eaton, E., Simone, C. B., et al. Mediboost: a patient stratification tool for interpretable decision making in the era of precision medicine. *Scientific Reports*, 6, 2016.
- Van Assche, A. and Blockeel, H. Seeing the forest through the trees. In *ILP*, 2007.
- Vandewiele, G., Janssens, O., Ongenaes, F., De Turck, F., and Van Hoecke, S. Genesim: genetic extraction of a single, interpretable model. *arXiv:1611.05722*, 2016.
- Wang, F. and Rudin, C. Falling rule lists. In *AISTATS*, 2015.
- Wolberg, W. H. and Mangasarian, O. L. Multisurface method of pattern separation for medical diagnosis applied to breast cytology. *Proceedings of the national academy of sciences*, 87(23):9193–9196, 1990.
- Yang, H., Rudin, C., and Seltzer, M. Scalable bayesian rule lists. In *ICML*, 2017.

A. Proofs of Main Results

In this section, we give a proof of Theorem 3.4.

A.1. Proof Overview

At a high level, the idea behind our proof of Theorem 3.4 is to show that the internal structure of T converges to that of T^* . Intuitively, this result holds because as we estimate T a larger and larger number of samples, the parameters (i, t) of each internal node of T and the parameters (y) of each leaf node of T should converge to the parameters of T^* . As long as the internal node parameters converge, then an input $x \in \mathcal{X}$ should be routed to leaf nodes in T and T^* at the same position. Then, as long as the internal node parameters converge, then x should furthermore be assigned the same label by T and T^* .

The key challenge is that the internal node parameter t is continuous, so T always has some error compared to T^* . Thus, to prove Theorem 3.4, we have to quantify this error and show that it goes to zero as n goes to infinity. Intuitively, we quantify this error as the probability that an input is routed to the wrong leaf node in T .

Our main lemma formalizes this notion. We begin by establishing some notation. Consider a node N^* in the exact greedy decision tree T^* . We define the function $\phi : T^* \rightarrow T$ to map N^* to the node $N = \phi(N^*)$ at the corresponding position in the estimated greedy decision tree T estimated using n samples. Now, given an input $x \in \mathcal{X}$, we write $x \xrightarrow{T^*} N^*$ if x is routed to node N^* in T^* , and similarly $x \xrightarrow{T} N$ if x is routed to node N in T . Finally, we denote the leaves of T^* and T by $\text{leaves}(T^*)$ and $\text{leaves}(T)$, respectively.

Then, we have the following key result:

Lemma A.1. *Let $p(x)$ be the probability density function for the distribution \mathcal{P} , let $N^* \in T^*$ and $N = \phi(N^*)$, and let*

$$\begin{aligned} p_{N^*}(x) &= p(x) \cdot \mathbb{I}[x \xrightarrow{T^*} N^*] \\ p_N(x) &= p(x) \cdot \mathbb{I}[x \xrightarrow{T} N]. \end{aligned}$$

Then, $\|p_N - p_{N^}\|_1$ converges in probability to 0 (where the randomness is taken over the n samples used to extract T), i.e., for any $\epsilon, \delta > 0$, there exists $n > 0$ such that*

$$\|p_N - p_{N^*}\|_1 \leq \epsilon$$

with probability at least $1 - \delta$.

Intuitively, p_{N^*} captures the distribution of points that are routed to N^* in T^* , and p_N captures the distribution of points that are routed to N in T . Then, this lemma says that the distribution of points routed to N^* and N are similar. We prove this lemma in Section A.3.

A.2. Proof of Main Theorem

We now use Lemma A.1 to prove Theorem 3.4. In particular, we must show that the quantity $P = \Pr_{x \sim \mathcal{P}}[T(x) \neq T^*(x)]$ is bounded by ϵ with probability at least $1 - \delta$. Throughout the proof, we use Lemma A.1 with parameters $(\frac{\epsilon}{K}, \frac{\delta}{2K})$, i.e., we have $\|p_N - p_{N^*}\|_1 \leq \frac{\epsilon}{K}$ with probability at least $1 - \frac{\delta}{2K}$. By a union bound, this fact holds for every leaf node in T^* with probability at least $1 - \frac{\delta}{2}$.

Then, our proof proceeds in two steps:

1. We show that a leaf node $N \in T$ is correctly labeled as long as ϵ is sufficiently small. More precisely, let $N^* \in \text{leaves}(T^*)$ such that $N^* = (y^*)$, and let $N = \phi(N^*) \in \text{leaves}(T)$ such that $N = (y)$; then, we show that for any $\delta' > 0$, there exists $n \in \mathbb{N}$ such that $y = y^*$ with probability at least $1 - \delta'$ (where the randomness is taken over the n samples used to extract T).
2. Using the Lemma A.1 together with the first step, we show that $P \leq \epsilon$ with probability at least $1 - \delta$.

Proving $y = y^*$. Let $p(x)$ be the probability density function for the distribution \mathcal{P} , and let $N^* \in \text{leaves}(T^*)$ such that $N^* = (y^*)$ and $N = \phi(N^*) \in \text{leaves}(T)$ such that $N = (y)$. First, we rewrite the objective (3) in terms of p_{N^*} . In

particular, for each $y' \in \mathcal{Y}$, let

$$\begin{aligned} p_{y'}^* &= \Pr_{x \sim \mathcal{P}}[f(x) = y' \wedge (x \xrightarrow{T^*} N^*)] \\ &= \int \mathbb{I}[f(x) = y'] \cdot \mathbb{I}[x \xrightarrow{T^*} N^*] \cdot p(x) dx. \end{aligned}$$

Then, we have $y^* = \arg \max_{y' \in \mathcal{Y}} p_{y'}^*$, since the denominator $\Pr_{x \sim \mathcal{P}}[x \xrightarrow{T^*} N^*]$ in (3) is constant with respect to y' . Similarly, we rewrite the objective (3) in terms of p_{N^*} , letting

$$p_{y'} = \frac{1}{n} \sum_{j=1}^n \mathbb{I}[f(x^{(j)}) = y'] \cdot \mathbb{I}[x^{(j)} \xrightarrow{T} N]$$

for each $y' \in \mathcal{Y}$, in which case we have $y = \arg \max_{y' \in \mathcal{Y}} p_{y'}$.

By Assumption 3.2, we know that y^* is the unique maximizer of $p_{y'}^*$, i.e.,

$$\Delta = p_{y^*}^* - \arg \max_{y' \neq y^*} p_{y'}^* > 0.$$

Therefore, to show that $y = y^*$, it suffices to show that for each $y' \in \mathcal{Y}$, we have

$$|p_{y'} - p_{y'}^*| \leq \frac{\Delta}{3},$$

since then, for each $y' \in \mathcal{Y}$, we have

$$p_{y^*} - p_{y'} \geq \left(p_{y^*}^* - \frac{\Delta}{3}\right) - \left(p_{y'}^* + \frac{\Delta}{3}\right) \geq \frac{\Delta}{3} > 0,$$

which implies that $y = y^*$ since y^* is the maximizer of $p_{y'}$.

To show that $|p_{y'} - p_{y'}^*| \leq \Delta/3$, we first define

$$\tilde{p}_{y'} = \int \mathbb{I}[f(x) = y'] \cdot \mathbb{I}[x \xrightarrow{T} N] \cdot p(x) dx.$$

Then, we have

$$|p_{y'} - p_{y'}^*| \leq |p_{y'} - \tilde{p}_{y'}| + |\tilde{p}_{y'} - p_{y'}^*|.$$

To bound the first term, let

$$d_{y'} = \mathbb{I}[f(x) = y'] \cdot \mathbb{I}[x \xrightarrow{T} N]$$

be a Bernoulli random variable, so

$$d_{y'}^{(j)} = \mathbb{I}[f(x^{(j)}) = y'] \cdot \mathbb{I}[x^{(j)} \xrightarrow{T} N]$$

are samples of $d_{y'}$ for $j \in [n]$. Then, we have $\tilde{p}_{y'} = \mathbb{E}[d_{y'}]$ and $p_{y'} = n^{-1} \sum_{j=1}^n d_{y'}^{(j)}$, so we can apply Hoeffding's inequality to get

$$\Pr \left[|p_{y'} - \tilde{p}_{y'}| > \frac{\Delta}{6} \right] \leq 2 \exp \left(-\frac{n\Delta^2}{18} \right).$$

To bound the second term, note that

$$\begin{aligned} |\tilde{p}_{y'} - p_{y'}^*| &= \left| \int \mathbb{I}[f(x) = y'] \cdot (\mathbb{I}[x \xrightarrow{T} N] - \mathbb{I}[x \xrightarrow{T^*} N^*]) \cdot p(x) dx \right| \\ &\leq \int |\mathbb{I}[x \xrightarrow{T} N] - \mathbb{I}[x \xrightarrow{T^*} N^*]| \cdot p(x) dx \\ &= \|p_N - p_{N^*}\|_1 \\ &\leq \epsilon. \end{aligned}$$

Finally, assume that $\epsilon < \Delta/6$; then, taking a union bound over $y' \in \mathcal{Y}$, we have that

$$|p_{y'} - p_{y'}^*| \leq \frac{\Delta}{3}$$

for all $y' \in \mathcal{Y}$ with probability at least $1 - \delta'$, where

$$\delta' = 2 \cdot |\mathcal{Y}| \cdot \exp\left(-\frac{n\Delta^2}{18}\right).$$

In particular, it follows that $y = y^*$ with probability at least $1 - \delta'$.

Bounding P . First, we separate the contribution of each leaf node to P :

$$\begin{aligned} P &= \Pr_{x \sim \mathcal{P}}[T(x) \neq T^*(x)] \\ &= \sum_{N^* \in \text{leaves}(T^*)} \Pr_{x \sim \mathcal{P}}[T(x) \neq T^*(x) \text{ and } x \xrightarrow{T^*} N^*]. \end{aligned}$$

Next, we apply the result from the first step of this proof with parameter $\delta' = \frac{\delta}{2K}$ (where K is the number of nodes in each T^* and T); then, for any leaf node $N^* \in \text{leaves}(T^*)$, the label assigned to N^* equals the label assigned to N with probability at least $1 - \frac{\delta}{2K}$. Taking a union bound over the leaf nodes, this fact holds true for all the leaf nodes with probability at least $1 - \frac{\delta}{2}$. For the remainder of the proof, we assume that this fact holds.

Consider an input x such that $x \xrightarrow{T^*} N^*$, as long as N^* and $\phi(N^*)$ have the same label, and additionally $x \xrightarrow{T} \phi(N^*)$, then $T(x) = T^*(x)$. Thus, we have

$$\Pr_{x \sim \mathcal{P}}[T(x) \neq T^*(x) \text{ and } x \xrightarrow{T^*} N^*] \leq \Pr_{x \sim \mathcal{P}}[\neg(x \xrightarrow{T} \phi(N^*)) \text{ and } x \xrightarrow{T^*} N^*].$$

As a consequence, we have

$$\begin{aligned} P &\leq \sum_{N^* \in \text{leaves}(T^*)} \Pr_{x \sim \mathcal{P}}[\neg(x \xrightarrow{T} \phi(N^*)) \text{ and } x \xrightarrow{T^*} N^*] \\ &= \sum_{N^* \in \text{leaves}(T^*)} \int (1 - \mathbb{I}[x \xrightarrow{T} \phi(N^*)]) \cdot \mathbb{I}[x \xrightarrow{T^*} N^*] \cdot p(x) dx. \end{aligned}$$

Now, we claim that

$$(1 - \mathbb{I}[x \xrightarrow{T} \phi(N^*)]) \cdot \mathbb{I}[x \xrightarrow{T^*} N^*] \leq |\mathbb{I}[x \xrightarrow{T^*} N^*] - \mathbb{I}[x \xrightarrow{T} \phi(N^*)]|.$$

To see this claim, note that both sides of inequality take values in $\{0, 1\}$. Furthermore, the right-hand side equals 0 only if the two indicators are equal. In this case, the left-hand side also equals 0, so the claim follows. Thus, we have

$$\begin{aligned} P &\leq \sum_{N^* \in \text{leaves}(T^*)} \int |\mathbb{I}[x \xrightarrow{T^*} N^*] - \mathbb{I}[x \xrightarrow{T} \phi(N^*)]| \cdot p(x) dx \\ &= \sum_{N^* \in \text{leaves}(T^*)} \int |\mathbb{I}[x \xrightarrow{T^*} N^*] \cdot p(x) - \mathbb{I}[x \xrightarrow{T} \phi(N^*)] \cdot p(x)| dx \\ &= \sum_{N^* \in \text{leaves}(T^*)} \|p_{\phi(N^*)} - p_{N^*}\|_1. \end{aligned}$$

By Lemma A.1, we have

$$P \leq \sum_{N^* \in \text{leaves}(T^*)} \frac{\epsilon}{K} \leq \epsilon.$$

Since Lemma A.1 holds with probability at least $1 - \frac{\delta}{2}$, and the first part of this proof holds with probability at least $1 - \frac{\delta}{2}$, by a union bound, we have $P \leq \epsilon$ with probability at least $1 - \delta$, which completes the proof.

A.3. Proof of Main Lemma

The key idea behind proving Lemma A.1 is to use induction on the structure of the tree. More precisely, it is clear that Lemma A.1 holds for the root node N_{T^*} of T^* , since every input is routed to the root, i.e.,

$$\mathbb{I}[x \xrightarrow{T^*} N_{T^*}] = \mathbb{I}[x \xrightarrow{T} \phi(N_{T^*})] = 1$$

for all $x \in \mathcal{X}$. Then, it suffices to show that if Lemma A.1 holds for the parent of a node $N^* \in T^*$, then it holds for N^* as well.

More precisely, let M^* be the parent of N^* , and let $M = \phi(M^*)$ be the parent of $N = \phi(N^*)$. Our goal is to prove that, assuming

$$\|p_M - p_{M^*}\|_1 \xrightarrow{P} 0,$$

then

$$\|p_N - p_{N^*}\|_1 \xrightarrow{P} 0$$

as well (note that we use \xrightarrow{P} to denote convergence in probability).

For simplicity, we prove the one-dimensional case, i.e., $\mathcal{X} = \mathbb{R}$. Proving the general case is a straightforward extension of our proof, but requires extra bookkeeping that obscures the key ideas. In particular, let $N^* \in T^*$ have form $N^* = (i^*, t^*)$, and let $N = \phi(N^*) \in T$ have form $N = (i, t)$. When $d = 1$, we know that $i = i^* = 1$, so we only have to prove that t converges to t^* . Proving that i converges to i^* is straightforward since there are only finitely many choices for i . With this restriction, we can assume that internal nodes have only a single parameter, i.e., $N^* = (t^*)$ where $t^* \in \mathbb{R}$, and $N = \phi(N^*) = (t)$ where $t \in \mathbb{R}$.

We begin our proof by expressing p_N in terms of p_M . We assume without loss of generality that N is the left child of M . Then, note that

$$\mathbb{I}[x \xrightarrow{T} N] = \mathbb{I}[x \xrightarrow{T} M] \cdot \mathbb{I}[x \leq t],$$

where $M = (t)$, so we have

$$p_N(x) = p_M(x) \cdot \mathbb{I}[x \leq t].$$

Now, our proof proceeds in two steps:

1. First, we show assuming $\|p_M - p_{M^*}\|_1 \xrightarrow{P} 0$, then $t \xrightarrow{P} t^*$.
2. Second, we show that assuming $t \xrightarrow{P} t^*$, then $\|p_N - p_{N^*}\|_1 \xrightarrow{P} 0$.

Step 1: Proving $t \xrightarrow{P} t^*$. First, we show that $\|p_M - p_{M^*}\|_1 \xrightarrow{P} 0$ implies

$$\|G - G^*\|_\infty \xrightarrow{P} 0,$$

where

$$\begin{aligned} G^*(s) &= G(i, s; \mathcal{P} \mid C_{M^*}) \\ G(s) &= G(i, s; \mathcal{P}_M) \end{aligned}$$

are the gain functions for T^* and T , respectively, where $G(i, s; \mathcal{Q})$ is defined in (2); as noted above, we have assumed $i = 1$ is a constant to simplify our exposition. Proving this step depends on the gain function being used to train the decision tree; we show that it holds for the gain function based on the Gini impurity in Lemma B.1.

Next, we show that as long as $\|G - G^*\|_\infty$ is sufficiently small, then the difference between their corresponding maximizers

$$\begin{aligned} t^* &= \arg \max_s G^*(s) \\ t &= \arg \max_s G(s) \end{aligned}$$

is small as well, i.e., $t \xrightarrow{P} t^*$.

By Assumption 3.2, we can prove the existence of a *gap*, which intuitively is an interval around t^* outside of which the $G^*(s)$ is “sufficiently smaller” than $G^*(t^*)$. More precisely:

Definition A.2. We say that a function $g : \mathbb{R} \rightarrow \mathbb{R}$ is (ϵ, δ) -gapped if it has a unique maximizer $s^* = \arg \max_{s \in \mathbb{R}} g(s)$, and for every $s \in \mathbb{R}$ such that $|s - s^*| > \epsilon$, we have $g(s^*) > g(s) + \delta$.

We show that as long as G^* is continuous and has bounded support, then for any $\epsilon' > 0$, there exists $\delta' > 0$ such that G^* is (ϵ', δ') -gapped; in Lemma B.3, we show that the gain function G^* based on the Gini impurity satisfies these technical assumptions. Then, let s_{\max} be a bound on the support of G^* , i.e., $G^*(s) = 0$ if $|s| > s_{\max}$. Let $\epsilon' > 0$ be arbitrary, and let

$$A_{\epsilon'} = \{s \in \mathbb{R} \mid |s| \leq s_{\max} \text{ and } |s - s^*| \geq \epsilon'\}.$$

Note that $A_{\epsilon'}$ is a compact set, so G^* achieves its maximum on $A_{\epsilon'}$, i.e.,

$$t_{\epsilon'}^* = \arg \max_{s \in A_{\epsilon'}} G^*(s).$$

Then, G^* is (ϵ', δ') -gapped, where

$$\delta' = \frac{G^*(t^*) - G^*(t_{\epsilon'}^*)}{2} > 0.$$

Note that we divide by 2 since the inequality in Definition A.2 is strict.

Now, we show that having a gap implies $t \xrightarrow{P} t^*$. In particular, suppose that $\|G^* - G\|_{\infty} \leq \frac{\delta'}{2}$. Then, we have

$$\begin{aligned} G^*(t^*) - G^*(t) &\leq \left(G(t^*) + \frac{\delta'}{2}\right) - \left(G(t) - \frac{\delta'}{2}\right) \\ &\leq G(t^*) - G(t) + \delta' \\ &\leq \delta', \end{aligned}$$

where the last step follows since t is the maximizer of G . In particular, we have shown that $|G^*(t^*) - G^*(t)| \leq \delta'$, so since G^* is (ϵ', δ') -gapped, it follows that $|t - t^*| \leq \epsilon'$. Since $\|G^* - G\|_{\infty} \xrightarrow{P} 0$, it follows that $t \xrightarrow{P} t^*$.

Step 2: Proving $\|p_N - p_{N^*}\|_1 \xrightarrow{P} 0$. Note that

$$\begin{aligned} \|p_N - p_{N^*}\|_1 &= \int |p_N(x) - p_{N^*}(x)| dx \\ &= \int |p_M(x) \cdot \mathbb{I}[x \leq t] - p_{M^*}(x) \cdot \mathbb{I}[x \leq t^*]| dx \\ &= \int |p_M(x) \cdot \mathbb{I}[x \leq t] - (p_M(x) + p_{M^*}(x) - p_M(x)) \cdot \mathbb{I}[x \leq t^*]| dx \\ &\leq \int p_M(x) \cdot |\mathbb{I}[x \leq t] - \mathbb{I}[x \leq t^*]| dx + \int |p_M(x) - p_{M^*}(x)| \cdot \mathbb{I}[x \leq t^*] dx. \end{aligned}$$

Assume without loss of generality that $t \leq t^*$. Then, for the first integral, note that the integrand equals 0 for $x \notin [t, t^*]$ and equals 1 for $x \in [t, t^*]$. Thus,

$$\begin{aligned} \int p_M(x) \cdot |\mathbb{I}[x \leq t] - \mathbb{I}[x \leq t^*]| dx &= \int p_M(x) \cdot \mathbb{I}[t \leq x \leq t^*] dx \\ &= \int_t^{t^*} p_M(x) dx \\ &\leq |t - t^*| \cdot p_{\max}, \end{aligned}$$

where the last step follows by Assumption 3.1, which says that $p(x) \leq p_{\max}$ for all $x \in \mathbb{R}$.

Next, for the second integral, note that

$$\int |p_M(x) - p_{M^*}(x)| \cdot \mathbb{I}[x \leq t^*] dx \leq \|p_M - p_{M^*}\|_1.$$

Together, we have

$$\|p_N - p_{N^*}\|_1 \leq \|p_M - p_{M^*}\|_1 + |t - t^*| \cdot p_{\max}.$$

Since the left-hand side converges in probability to 0, so does the right-hand side, as claimed.

B. Proof of Technical Lemmas

In this section, we prove the technical lemmas required for our proofs of Lemma A.1 and Theorem 3.4.

B.1. Proof of Convergence of the Gain Function

In this section, we prove that the gain function G converges uniformly to G^* as $n \rightarrow \infty$. To simplify notation, we use slightly different notation for the Gini impurity H compared to the definition in (2).

Lemma B.1. *Let*

$$\begin{aligned} G^*(t) &= -H^*(f, C_{N^*} \wedge (x \leq t)) - H^*(f, C_{N^*} \wedge (x > t)) + H^*(f, C_{N^*}) \\ H^*(f, C) &= \left(1 - \sum_{y \in \mathcal{Y}} \left(\frac{\Pr_{x \sim \mathcal{P}}[f(x) = y \wedge C]}{\Pr_{x \sim \mathcal{P}}[C]} \right)^2 \right) \cdot \Pr_{x \sim \mathcal{P}}[C] \end{aligned}$$

be the gain function based on the Gini impurity for the exact greedy decision tree, and let

$$\begin{aligned} G(t) &= -H(f, C_N \wedge (x \leq t)) - H(f, C_N \wedge (x > t)) + H(f, C_N) \\ H(f, C) &= \left(1 - \sum_{y \in \mathcal{Y}} \left(\frac{\frac{1}{n} \sum_{j=1}^n \mathbb{I}[f(x^{(j)}) = y \wedge x^{(j)} \in \mathcal{F}(C)]}{\frac{1}{n} \sum_{j=1}^n \mathbb{I}[x^{(j)} \in \mathcal{F}(C)]} \right)^2 \right) \cdot \frac{1}{n} \sum_{j=1}^n \mathbb{I}[x^{(j)} \in \mathcal{F}(C)] \end{aligned}$$

be the corresponding gain function for the estimated greedy decision tree.

If $\|p_N - p_{N^*}\|_1 \xrightarrow{P} 0$, where

$$\begin{aligned} p_{N^*}(x) &= p(x) \cdot \mathbb{I}[x \xrightarrow{T^*} N^*] \\ p_N(x) &= p(x) \cdot \mathbb{I}[x \xrightarrow{T} N], \end{aligned}$$

then we have $\|G - G^*\|_\infty \xrightarrow{P} 0$.

Proof. First, note that

$$\begin{aligned} \|G - G^*\|_\infty &\leq \sup_{t \in \mathbb{R}} |H^*(f, C_{N^*} \wedge (x \leq t)) - H(f, C_N \wedge (x \leq t))| \\ &\quad + \sup_{t \in \mathbb{R}} |H^*(f, C_{N^*} \wedge (x > t)) - H(f, C_N \wedge (x > t))| \\ &\quad + \sup_{t \in \mathbb{R}} |H^*(f, C_{N^*}) - H(f, C_N)|. \end{aligned}$$

We prove that the first term converges in probability to 0 as $n \rightarrow \infty$; the remaining two terms can be bounded using the same argument. In particular, let

$$\begin{aligned} H^*(t) &= H^*(f, C_{N^*} \wedge (x \leq t)) \\ H(t) &= H(f, C_N \wedge (x \leq t)), \end{aligned}$$

so our goal is to show that $\|H - H^*\|_\infty \xrightarrow{p} 0$. To simplify our expressions, define

$$\begin{aligned} g^*(t) &= \Pr_{x \sim \mathcal{P}}[x \in \mathcal{F}(C_{N^*} \wedge (x \leq t))] \\ h_y^*(t) &= \Pr_{x \sim \mathcal{P}}[f(x) = y \wedge x \in \mathcal{F}(C_{N^*} \wedge (x \leq t))] \\ g(t) &= \frac{1}{n} \sum_{j=1}^n \mathbb{I}[x^{(j)} \in \mathcal{F}(C_N \wedge (x \leq t))] \\ h_y(t) &= \frac{1}{n} \sum_{j=1}^n \mathbb{I}[f(x^{(j)}) = y \wedge x^{(j)} \in \mathcal{F}(C_N \wedge (x^{(j)} \leq t))], \end{aligned}$$

A useful fact is that

$$\begin{aligned} 0 &\leq h_y^*(t) \leq g^*(t) \leq 1 \\ 0 &\leq h_y(t) \leq g(t) \leq 1 \end{aligned}$$

for all $t \in \mathbb{R}$ and all $y \in \mathcal{Y}$ (but assuming the random samples $x^{(j)}$ are fixed). Now, we have

$$\begin{aligned} H^*(t) &= \left(1 - \sum_{y \in \mathcal{Y}} \left(\frac{h_y^*(t)}{g^*(t)}\right)^2\right) \cdot g^*(t) \\ &= g^*(t) - \sum_{y \in \mathcal{Y}} \frac{h_y^*(t)^2}{g^*(t)}, \end{aligned}$$

and similarly

$$H(t) = g(t) - \sum_{y \in \mathcal{Y}} \frac{h_y(t)^2}{g(t)}.$$

Then, we have

$$\|H - H^*\|_\infty \leq \sup_{t \in \mathbb{R}} |g(t) - g^*(t)| + \sum_{y \in \mathcal{Y}} \sup_{t \in \mathbb{R}} \left| \frac{h_y^*(t)^2}{g^*(t)} - \frac{h_y(t)^2}{g(t)} \right|.$$

We show that for a fixed $y \in \mathcal{Y}$, we have

$$\sup_{t \in \mathbb{R}} \left| \frac{h_y^*(t)^2}{g^*(t)} - \frac{h_y(t)^2}{g(t)} \right| \xrightarrow{p} 0. \quad (4)$$

Bounding the first term of $\|H - H^*\|_\infty$ follows similarly; together, these limits imply that $\|H - H^*\|_\infty \xrightarrow{p} 0$ as well. We break the remainder of the proof into two steps:

1. First, we prove that $\|g - g^*\|_\infty \xrightarrow{p} 0$ and $\|h_y - h_y^*\|_\infty \xrightarrow{p} 0$.
2. Second, we use the first part to show that (4) holds.

Step 1. We prove that $\|h_y - h_y^*\|_\infty \xrightarrow{p} 0$; the claim $\|g - g^*\|_\infty \xrightarrow{p} 0$ follows similarly. First, note that

$$\begin{aligned} h_y^*(t) &= \int \mathbb{I}[f(x) = y] \cdot \mathbb{I}[x \xrightarrow{N^*} T^*] \cdot \mathbb{I}[x \leq t] \cdot p(x) dx \\ &= \int \mathbb{I}[f(x) = y] \cdot \mathbb{I}[x \leq t] \cdot p_{N^*}(x) dx, \end{aligned}$$

and define

$$\tilde{h}_y(t) = \int \mathbb{I}[f(x) = y] \cdot \mathbb{I}[x \leq t] \cdot p_N(x) dx.$$

Then, note that

$$\|h_y - h_y^*\|_\infty \leq \|h_y - \tilde{h}_y\|_\infty + \|\tilde{h}_y - h_y^*\|_\infty.$$

Bounding the first term, which represents the estimation error, is somewhat involved, so we relegate the proof to another lemma. In particular, taking $g = h_y$ and $g^* = \tilde{h}_y$ in Lemma B.2, it follows that $\|h_y - \tilde{h}_y\|_\infty \xrightarrow{p} 0$.

To bound the second term, note that

$$\begin{aligned} \|\tilde{h}_y - h_y^*\|_\infty &= \sup_{t \in \mathbb{R}} \left| \int \mathbb{I}[f(x) = y] \cdot \mathbb{I}[x \leq t] \cdot (p_N(x) - p_{N^*}(x)) dx \right| \\ &\leq \sup_{t \in \mathbb{R}} \int |p_N(x) - p_{N^*}(x)| dx \\ &= \|p_N - p_{N^*}\|_1 \\ &\xrightarrow{p} 0, \end{aligned}$$

where the last step follows by our assumption.

Step 2. Let $\epsilon, \delta > 0$ be arbitrary. We need to show that

$$\left| \frac{h_y^*(t)^2}{g^*(t)} - \frac{h_y(t)^2}{g(t)} \right| \leq \epsilon$$

for every $t \in \mathbb{R}$ with probability at least $1 - \delta$. By the previous step, we can take

$$\begin{aligned} \|g - g^*\|_\infty &\leq \frac{\epsilon}{8} \\ \|h_y - h_y^*\|_\infty &\leq \frac{\epsilon^2}{16} \end{aligned}$$

each with probability at least $1 - \frac{\delta}{2}$, so by a union bound, both these inequalities hold with probability at least $1 - \delta$.

We consider two cases. First, suppose that $g^*(t) \leq \frac{\epsilon}{4}$, in which case

$$g(t) \leq g^*(t) + \frac{\epsilon}{8} \leq \frac{\epsilon}{2}.$$

Then, since $h_y^*(t) \leq g^*(t)$ and $h_y(t) \leq g(t)$, we have

$$\begin{aligned} \left| \frac{h_y^*(t)^2}{g^*(t)} - \frac{h_y(t)^2}{g(t)} \right| &\leq \left| \frac{h_y^*(t)^2}{g^*(t)} \right| + \left| \frac{h_y(t)^2}{g(t)} \right| \\ &\leq |g^*(t)| + |g(t)| \\ &\leq \epsilon. \end{aligned}$$

One detail is that when $g^*(t) = 0$, then $H^*(t)$ is not well-defined. Defining $H^*(t) = 0$ in this case is standard practice, since $h_y^*(t) \leq g^*(t)$, so

$$H^*(t) = \frac{h_y^*(t)^2}{g^*(t)} \leq \frac{g^*(t)^2}{g^*(t)} \leq g^*(t) = 0.$$

Similarly, we define $H(t) = 0$ if $g(t) = 0$. In either case, the above argument still applies.

Second, suppose that $g^*(t) \geq \frac{\epsilon}{4}$, in which case

$$g(t) \geq g^*(t) - \frac{\epsilon}{8} \geq \frac{\epsilon}{8}.$$

Then, we have

$$\begin{aligned}
 \left| \frac{h_y^*(t)^2}{g^*(t)} - \frac{h_y(t)^2}{g(t)} \right| &\leq \frac{8}{\epsilon} \cdot |h_y^*(t)^2 - h_y(t)^2| \\
 &= \frac{8}{\epsilon} \cdot |h_y^*(t) - h_y(t)| \cdot |h_y^*(t) + h_y(t)| \\
 &\leq \frac{8}{\epsilon} \cdot \frac{\epsilon^2}{16} \cdot 2 \\
 &\leq \epsilon.
 \end{aligned}$$

In either case, the claim follows, completing the proof. \square

Next, we prove that the estimation error in Lemma B.1 goes to zero.

Lemma B.2. Let \mathcal{P} be a probability distribution over \mathbb{R} , let $p(x)$ be the probability density function for \mathcal{P} , let $F(x)$ be the cumulative distribution function for \mathcal{P} , let $\alpha : \mathbb{R} \rightarrow [0, 1]$ be an arbitrary function, let

$$g^*(t) = \int \alpha(x) \cdot \mathbb{I}[x \leq t] \cdot p(x) dx,$$

and let $x^{(1)}, \dots, x^{(n)}$ be i.i.d. random samples from \mathcal{P} , and let

$$g(t) = \frac{1}{n} \sum_{j=1}^n \alpha(x^{(j)}) \cdot \mathbb{I}[x^{(j)} \leq t]$$

be the empirical estimate of g^* on these samples. Then, we have

$$\Pr_{x^{(1)}, \dots, x^{(n)} \sim \mathcal{P}} \left[\|g - g^*\|_\infty \geq \frac{4 \log n}{\sqrt{n}} \right] \leq \frac{2}{n^{3/2}},$$

for sufficiently large n .

Proof. First, we define points $t_0, t_1, \dots, t_{\sqrt{n}} \in \mathbb{R}$ that divide \mathbb{R} into \sqrt{n} intervals according to the cumulative distribution function $F(x)$ (for convenience, we assume n is a perfect square). In particular, we choose t_i to satisfy

$$t_i \in F^{-1} \left(\frac{i}{\sqrt{n}} \right).$$

For convenience, we choose $t_0 = -\infty$ and $t_{\sqrt{n}} = \infty$, which satisfy the condition. Now, for each $i \in [\sqrt{n}]$, let $I_i = (t_{i-1}, t_i]$. Note that these intervals cover \mathbb{R} , i.e., $\mathbb{R} = I_1 \cup \dots \cup I_{\sqrt{n}}$.

Then, we can decompose the quantity $\|g - g^*\|_\infty$ into three parts:

$$\begin{aligned}
 \|g - g^*\|_\infty &= \sup_{t \in \mathbb{R}} |g(t) - g^*(t)| \\
 &= \sup_{i \in [\sqrt{n}]} \sup_{t \in I_i} |g(t) - g^*(t)| \\
 &\leq \sup_{i \in [\sqrt{n}]} \sup_{t \in I_i} \{|g(t) - g(t_i)| + |g(t_i) - g^*(t_i)| + |g^*(t_i) - g^*(t)|\} \\
 &\leq \sup_{i \in [\sqrt{n}]} \sup_{t \in I_i} |g(t) - g(t_i)| + \sup_{i \in [\sqrt{n}]} |g(t_i) - g^*(t_i)| + \sup_{i \in [\sqrt{n}]} \sup_{t \in I_i} |g^*(t_i) - g^*(t)|.
 \end{aligned}$$

We show that each of these three parts can be made arbitrarily small with high probability by taking n sufficiently large.

First term. We first show that for every $i \in [\sqrt{n}]$, the interval I_i contains at most $n^{1/2} \log n$ of the points $x^{(1)}, \dots, x^{(n)}$ with high probability. By the definition of the points t_i , the probability that a single randomly selected point $x^{(j)}$ falls in I_i is $n^{-1/2}$ (since the points t_i were constructed according to the cumulative distribution function F):

$$M = \mathbb{E}_{x \sim \mathcal{P}} [\mathbb{I}[x \in I_i]] = \Pr_{x \sim \mathcal{P}}[x \in I_i] = \frac{1}{\sqrt{n}}.$$

Then, the fraction of the n points $x^{(j)}$ that fall in the interval I_i is

$$\hat{M} = \frac{1}{n} \sum_{j=1}^n \mathbb{I}[x^{(j)} \in I_i].$$

Note that each $\mathbb{I}[x^{(j)} \in I_i]$ is a random variable in $[0, 1]$, so by Hoeffding's inequality, we have

$$\Pr_{x^{(1)}, \dots, x^{(n)} \sim \mathcal{P}} \left[|\hat{M} - M| \geq \frac{2 \log n}{\sqrt{n}} \right] \leq 2e^{-2(\log n)^2} \leq \frac{1}{n^2}$$

for sufficiently large n . Now, note that each point $x^{(j)}$ in I_i can increase the value of $|g(t) - g(t_i)|$ by at most n^{-1} . Since there are $n \cdot \hat{M}$ points $x^{(j)}$ in I_i , the total increase is bounded by \hat{M} , i.e.,

$$\Pr_{x^{(1)}, \dots, x^{(n)} \sim \mathcal{P}} \left[\sup_{t \in I_i} |g(t) - g(t_i)| \geq \frac{2 \log n}{\sqrt{n}} \right] \leq \frac{1}{n^2}.$$

By a union bound, this inequality holds for every $i \in [\sqrt{n}]$ with probability $n^{-3/2}$.

Second term. Note that each $\alpha(x^{(j)}) \cdot \mathbb{I}[x^{(j)} \geq t]$ is a random variable in $[0, 1]$. Therefore, by the Hoeffding inequality, we have

$$\Pr_{x^{(1)}, \dots, x^{(n)} \sim \mathcal{P}} \left[|g(t_i) - g^*(t_i)| \geq \frac{\log n}{\sqrt{n}} \right] \leq 2e^{-2(\log n)^2} \leq \frac{1}{n^2}$$

for sufficiently large n . By a union bound, this inequality holds for every $i \in [\sqrt{n}]$ with probability $n^{-3/2}$.

Third term. Since $t \leq t_i$, we have $\mathbb{I}[x \leq t] \leq \mathbb{I}[x \leq t_i]$. Thus, for all $t \in I_i$, we have

$$\begin{aligned} |g^*(t_i) - g^*(t)| &= \left| \int \alpha(x) \cdot (\mathbb{I}[x \leq t_i] - \mathbb{I}[x \leq t]) \cdot p(x) dx \right| \\ &\leq \int (\mathbb{I}[x \leq t_i] - \mathbb{I}[x \leq t]) \cdot p(x) dx \\ &= F(t_i) - F(t) \\ &\leq n^{-1/2}, \end{aligned}$$

where the last inequality follows from the definition of t_i and the fact that $t \in I_i$.

Combined bound. Putting the three results together, we can conclude that for sufficiently large n , we have

$$\Pr_{x^{(1)}, \dots, x^{(n)} \sim \mathcal{P}} \left[\|g - g^*\|_\infty \geq \frac{4 \log n}{\sqrt{n}} \right] \leq \frac{2}{n^{3/2}},$$

as claimed. □

B.2. Proof of Regularity of the Gain Function

In this section, we prove that the gain function G^* satisfies certain regularity conditions.

Lemma B.3. *The function $G^* : \mathbb{R} \rightarrow \mathbb{R}$ is continuous and has bounded support.*

Proof. It is clear that G^* is continuous. To see that G^* has bounded support, recall that $p(x)$ has bounded support, i.e., $p(x) = 0$ for $|x| > x_{\max}$. Then, note that if $s > x_{\max}$, we have

$$\begin{aligned} \Pr_{x \sim \mathcal{P}}[C_{N^*} \wedge (x \leq s)] &= \Pr_{x \sim \mathcal{P}}[C_{N^*}] \\ \Pr_{x \sim \mathcal{P}}[C_{N^*} \wedge (x > s)] &= 0 \\ \Pr_{x \sim \mathcal{P}}[f(x) = y \mid C_{N^*} \wedge (x \leq s)] &= \Pr_{x \sim \mathcal{P}}[f(x) = y \mid C_{N^*}] \\ \Pr_{x \sim \mathcal{P}}[f(x) = y \mid C_{N^*} \wedge (x > s)] &= 0 \end{aligned}$$

Therefore, we have

$$G^*(s) = -H^*(f, C_{N^*} \wedge (x \leq s)) - H(f, C_{N^*} \wedge (x > s)) + H(f, C_{N^*}) = 0.$$

By a similar argument, $G^*(s) = 0$ for $s < -x_{\max}$, so the claim follows. □

C. User Study Interface

We include images of our user study on the following pages. Where applicable, the marked answers are the correct ones. Within each part, we randomized the order in which the decision tree and the rule list or decision set appeared.

Understanding Machine Learning Models

Thank you for taking the time to participate in this user study! Overall, we expect this user study to take about 15 minutes to complete. If you have any questions, feel free to email me at obastani@gmail.com.

Instructions

This study assumes that you have some familiarity with decision trees. We ask that you answer a series of questions based on four different models. The answers to these questions depend only on the structure of the model, not on any prior knowledge. While the models were trained on real data, their structure may not reflect reality (e.g., due to spurious correlations, covariate shift, etc.); please ignore any such issues when answering questions.

We expect that each question should take at most 1-2 minutes to answer. None of these questions are trick questions, so don't overthink them! If you are not able to determine the answer in about 2 minutes, please respond "Skip". Refreshing the page or hitting back will discard your answers.

Disclaimer

By submitting this form, you acknowledge that your participation in this study is voluntary, and that you are aware that you may choose to terminate your participation at any time for any reason without penalty. Your responses to this study will be kept confidential.

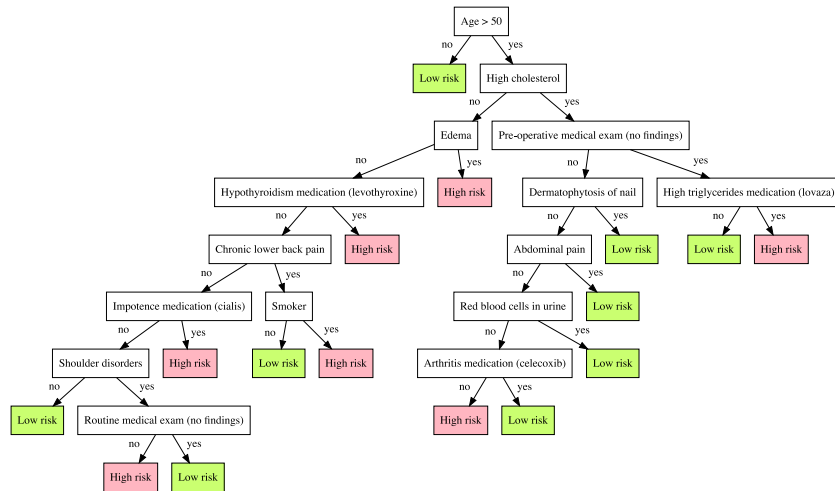
Part I: Predicting diabetes risk

Consider a machine learning model trained to predict diabetes risk (high vs. low) based on a patient's prior diagnoses, current prescribed medications, and demographic features.

Decision Tree

The following decision tree predicts diabetes risk; please use this model to answer the five following questions:

Interpreting Blackbox Models via Model Extraction



1. Consider patients over 50 years old who are otherwise healthy and are not taking any medications. According to the decision tree, are these patients at a high risk for diabetes?

- Yes
 No
 Skip

2. According to the decision tree, does being over 50 years old put patients at a relatively higher risk of diabetes?

- Yes
 No
 Skip

3. Consider patients over 50 years old who have high cholesterol, and have had a pre-operative medical exam with no findings. What additional information does the decision tree need to give an assessment of their diabetes risk?

- Whether they have edema
 Whether they have dermatophytosis of nail
 Whether they are taking high triglycerides medication
 No additional information is needed
 Skip

4. According to the decision tree, for which patient subpopulation might a diagnosis of chronic lower back pain newly introduce a high risk of diabetes?

- Patients who are over 50 years old
 Patients who are over 50 years old and have high cholesterol
 Patients who are over 50 years old and who smoke
 Skip

5. Smoking is known to increase risk of diabetes, so the local hospital has started a program to help smokers quit smoking. According to the decision tree, which patient subpopulation should we target in this program if we want to reduce diabetes risk?

- Patients over 50 years old who have high cholesterol

- Patients over 50 years old who have chronic lower back pain
- Patients over 50 years old who have high cholesterol, edema, chronic lower back pain, and who take medication for hypothyroidism
- Skip

Rule List

A rule list is a one-sided decision tree, which we visualize as an program consisting of a series of if-then-else statements. The following rule list predicts diabetes risk; please use this model to answer the five following questions:

```
if Age < 41 then Low risk
else if Moderate/severe pain medication (tramadol) then High risk
else if Arthritis medication (etodolac) then Low risk
else if High cholesterol and Smoker then High risk
else if High blood pressure then High risk
else if Age < 53 then Low risk
else if Restless legs syndrome then Low risk
else if not High cholesterol then Low risk
else High risk
```

1. Consider patients over 53 years old who are otherwise healthy and are not taking any medications. According to the rule list, are these patients at a high risk for diabetes?
 - Yes
 - No
 - Skip
2. According to the rule list, does being over 41 years old put patients at a relatively higher risk of diabetes?
 - Yes
 - No
 - Skip
3. Consider patients who are between 41 and 52 years old who are taking arthritis medication. What additional information does the rule list need to give an assessment of their diabetes risk?
 - Whether they are taking medication for moderate/severe pain
 - Whether they are taking medication for moderate/severe pain, whether they have high cholesterol, whether they have restless legs syndrome, and whether they smoke
 - Whether they have high blood pressure, and whether they smoke
 - No additional information is needed
 - Skip
4. According to the rule list, for which patient subpopulation might a diagnosis of high cholesterol newly introduce a high risk of diabetes?
 - Patients who are over 41 years old
 - Patients who are over 41 years old and take arthritis medication

- Patients who are over 41 years old who smoke
- Skip

5. Smoking is known to increase risk of diabetes, so the local hospital has started a program to help smokers quit smoking. According to the rule list, which patient subpopulation should we target in this program if we want to reduce diabetes risk?

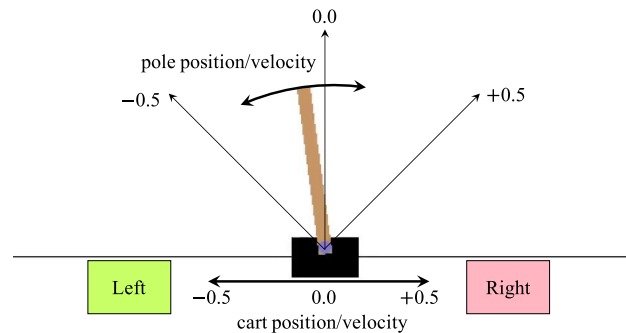
- Patients over 41 years old
- Patients over 41 years old who have high cholesterol
- Patients over 41 years old who have high cholesterol, and take medication for arthritis
- Skip

Miscellaneous

1. Which type of model did you find easier to understand?
- Decision tree
 - Rule list
 - Similar

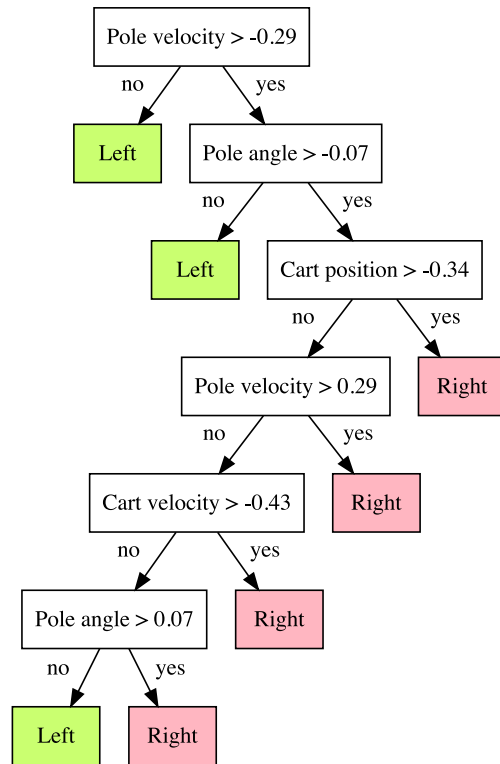
Part II: Cart-pole controller

Consider a machine learning model that controls a 2D cart, which can go left or right, with the goal of ensuring that the pole on top of the cart does not fall. The following cart-pole diagram below illustrates this system (the numbers shown are only for intuition); understanding this system may be helpful, but is not necessary for answering any of the questions in this study:



Decision Tree

The following decision tree was trained to control a cart-pole; please use this model to answer the three following questions:



1. Suppose that the pole velocity is 0.1, the pole angle is -0.2, and the cart position is 0.3. According to the decision tree, which action is taken?

- Left
- Right
- Skip

2. In theory, the action taken should not depend on the position of the cart. Does the decision tree satisfy this property?

- Yes
- No
- Skip

3. The cart-pole control problem is symmetric along the y-axis (i.e., left-to-right). More precisely, if we flip the sign of all the state variables (i.e., positions and velocities of cart and pole), then the resulting dynamics should be exactly the same (with a flipped sign). Is the decision tree symmetric along the y-axis (i.e., left-to-right) in an analogous way?

- Yes
- No
- Skip

Decision Set

A decision set is equivalent to a rule list, but uses a different training algorithm and is typically formatted slightly differently. In particular, the **else** keywords are implicit; i.e., when multiple **if**-rules trigger, then the topmost one applies. The following decision set was trained to control a cart-pole; please use this model to answer the three following questions:

```
if 0.29 < Pole angle < 0.86 then Left
if -1.29 < Cart velocity < -0.43 then Left
if 0.43 < Cart velocity < 1.29 then Left
if -0.34 < Cart position < 0.34 then Right
default Left
```

1. Suppose that the pole angle is 0.2, the cart velocity is 0.5, and the cart position is 0.3. According to the decision set, which action is taken?

- Left
- Right
- Skip

2. In theory, the action taken should not depend on the position of the cart. Does the decision set satisfy this property?

- Yes
- No
- Skip

3. The cart-pole control problem is symmetric along the y-axis (i.e., left-to-right). More precisely, if we flip the sign of all the state variables (i.e., positions and velocities of cart and pole), then the resulting dynamics should be exactly the same (with a flipped sign). Is the decision set symmetric along the y-axis (i.e., left-to-right) in an analogous way?

- Yes
- No
- Skip

Miscellaneous

1. Which type of model did you find easier to understand?

- Decision tree
- Decision set
- Similar

Part IV: Optional Information

Interpreting Blackbox Models via Model Extraction

Please let us know if you have any comments or suggestions (optional):

If you would like to hear about the results of our user study once complete, please give as an email address where we can contact you (optional):

Note: Upon submitting this form, you will be taken to a page asking if you trust a Google Apps Script created by obastani@gmail.com. You **do not** need to click the "TRUST APP" button; as long as you see the text "Your response has been recorded...", then your response will already have been recorded.